Improved Upper Limits on the Flavor-Changing Neutral Current Decays $B \rightarrow K\ell^+\ell^-$ and $B \rightarrow K^*(892)\ell^+\ell^-$

S. Anderson,[1] V. V. Frolov,[1] Y. Kubota,[1] S. J. Lee,[1] R. Poling,[1] A. Smith,[1] C. J. Stepaniak,[1] J. Urheim,[1] S. Ahmed,[2] M. S. Alam,[2] S. B. Athar,[2] L. Jian,[2] L. Ling,[2] M. Saleem,[2] S. Timm,[2] F. Wappler,[2] A. Anastassov,[3] E. Eckhart,[3] K. K. Gan,[3] C. Gwon,[3] T. Hart,[3] K. Honscheid,[3] D. Hufnagel,[3] H. Kagan,[3] R. Kass,[3] T. K. Pedlar,[3] J. B. Thayer,[3] E. von Toerne,[3] M. M. Zoeller,[3] S. J. Richichi,[4] H. Severini,[4] P. Skubic,[4] A. Undrus,[4] V. Savinov,[5] S. Chen,[6] J. W. Hinson,[6] J. Lee,[6] D. H. Miller,[6] E. I. Shibata,[6] I. P. J. Shipsey,[6] V. Pavlunin,[6] D. Cronin-Hennessy,[7] Y. Kwon,[7,*] A. L. Lyon,[7] W. Park,[7] E. H. Thorndike,[7] T. E. Coan,[8] Y. S. Gao,[8] Y. Maravin,[8] I. Narsky,[8] R. Stroynowski,[8] J. Ye,[8] T. Wlodek,[8] M. Artuso,[9] K. Benslama,[9] C. Boulahouache,[9] K. Bukin,[9] E. Dambasuren,[9] G. Majumder,[9] R. Mountain,[9] T. Skwarnicki,[9] S. Stone,[9] J. C. Wang,[9] A. Wolf,[9] S. Kopp,[10] M. Kostin,[10] A. H. Mahmood,[11] S. E. Csorna,[12] I. Danko,[12] K. W. McLean,[12] Z. Xu,[12] R. Godang,[13] G. Bonvicini,[14] D. Cinabro,[14] M. Dubrovin,[14] S. McGee,[14] A. Bornheim,[15] G. Eigen,[15,†] E. Lipeles,[15] S. P. Pappas,[15] A. Shapiro,[15] W. M. Sun,[15] A. J. Weinstein,[15] D. E. Jaffe,[16] R. Mahapatra,[16] G. Masek,[16] H. P. Paar,[16] A. Eppich,[17] R. J. Morrison,[17] R. A. Briere,[18] G. P. Chen,[18] T. Ferguson,[18] H. Vogel,[18] J. P. Alexander,[19] C. Bebek,[19] B. E. Berger,[19] K. Berkelman,[19] F. Blanc,[19] V. Boisvert,[19] D. G. Cassel,[19] P. S. Drell,[19] J. E. Duboscq,[19] K. M. Ecklund,[19] R. Ehrlich,[19] P. Gaidarev,[19] L. Gibbons,[19] B. Gittelman,[19] S. W. Gray,[19] D. L. Hartill,[19] B. K. Heltsley,[19] L. Hsu,[19] C. D. Jones,[19] J. Kandaswamy,[19] D. L. Kreinick,[19] M. Lohner,[19] A. Magerkurth,[19] H. Mahlke-Krüger,[19] T. O. Meyer,[19] N. B. Mistry,[19] E. Nordberg,[19] M. Palmer,[19] J. R. Patterson,[19] D. Peterson,[19] D. Riley,[19] A. Romano,[19] H. Schwarthoff,[19] J. G. Thayer,[19] D. Urner,[19] B. Valant-Spaight,[19] G. Viehhauser,[19] A. Warburton,[19] P. Avery,[20] C. Prescott,[20] A. I. Rubiera,[20] H. Stoeck,[20] J. Yelton,[20] G. Brandenburg,[21] A. Ershov,[21] D. Y.-J. Kim,[21] R. Wilson,[21] B. I. Eisenstein,[22] J. Ernst,[22] G. E. Gladding,[22] G. D. Gollin,[22] R. M. Hans,[22] E. Johnson,[22] I. Karliner,[22] M. A. Marsh,[22] C. Plager,[22] C. Sedlack,[22] M. Selen,[22] J. J. Thaler,[22] J. Williams,[22] K. W. Edwards,[23] A. J. Sadoff,[24] R. Ammar,[25] A. Bean,[25] D. Besson,[25] and X. Zhao[25]

(CLEO Collaboration)

[1] *University of Minnesota, Minneapolis, Minnesota 55455*
[2] *State University of New York at Albany, Albany, New York 12222*
[3] *The Ohio State University, Columbus, Ohio 43210*
[4] *University of Oklahoma, Norman, Oklahoma 73019*
[5] *University of Pittsburgh, Pittsburgh, Pennsylvania 15260*
[6] *Purdue University, West Lafayette, Indiana 47907*
[7] *University of Rochester, Rochester, New York 14627*
[8] *Southern Methodist University, Dallas, Texas 75275*
[9] *Syracuse University, Syracuse, New York 13244*
[10] *University of Texas, Austin, Texas 78712*
[11] *University of Texas–Pan American, Edinburg, Texas 78539*
[12] *Vanderbilt University, Nashville, Tennessee 37235*
[13] *Virginia Polytechnic Institute and State University, Blacksburg, Virginia 24061*
[14] *Wayne State University, Detroit, Michigan 48202*
[15] *California Institute of Technology, Pasadena, California 91125*
[16] *University of California, San Diego, La Jolla, California 92093*
[17] *University of California, Santa Barbara, California 93106*
[18] *Carnegie Mellon University, Pittsburgh, Pennsylvania 15213*
[19] *Cornell University, Ithaca, New York 14853*
[20] *University of Florida, Gainesville, Florida 32611*
[21] *Harvard University, Cambridge, Massachusetts 02138*
[22] *University of Illinois, Urbana-Champaign, Illinois 61801*
[23] *Carleton University, Ottawa, Ontario, Canada K1S 5B6*
and the Institute of Particle Physics, Canada
[24] *Ithaca College, Ithaca, New York 14850*
[25] *University of Kansas, Lawrence, Kansas 66045*

We have searched a sample of 9.6×10^6 $B\bar{B}$ events for the flavor-changing neutral current decays $B \rightarrow K\ell^+\ell^-$ and $B \rightarrow K^*(892)\ell^+\ell^-$. We subject the latter decay to the requirement that the dilepton mass $m_{\ell\ell}$ exceed 0.5 GeV. There is no indication of a signal. We obtain the 90% confidence level upper limits $\mathcal{B}(B \rightarrow K\ell^+\ell^-) < 1.7 \times 10^{-6}$ and $\mathcal{B}(B \rightarrow K^*(892)\ell^+\ell^-)_{m_{\ell\ell}>0.5 \text{ GeV}} < 3.3 \times 10^{-6}$. We also obtain

an upper limit on the weighted average $0.65\mathcal{B}(B \to K\ell^+\ell^-) + 0.35\mathcal{B}(B \to K^*(892)\ell^+\ell^-)_{m_{\ell\ell}>0.5 \text{ GeV}} < 1.5 \times 10^{-6}$. The weighted-average limit is only 50% above the standard model prediction.

The flavor-changing neutral current (FCNC) decay $b \to s\ell^+\ell^-$ is sensitive to physics beyond the standard model [1], and, like the radiative penguin decay $b \to s\gamma$, is more amenable to calculation than purely hadronic FCNC decays. The decay $b \to s\ell^+\ell^-$ depends on the magnitude and sign of the three Wilson coefficients C_7, C_9, and C_{10} in the effective Hamiltonian, while $b \to s\gamma$ depends only on the magnitude of C_7. These three Wilson coefficients are likely places for new physics to appear, as they come from loop and box diagrams. Upper limits on the branching fraction for $b \to s\ell^+\ell^-$ thus place constraints on new physics, while observation of $b \to s\ell^+\ell^-$ at a rate in excess of that predicted by the standard model would provide evidence for new physics. Just as we first observed $b \to s\gamma$ through its exclusive decay $B \to K^*(892)\gamma$ [2], and only later in an inclusive fashion [3], so we search for $b \to s\ell^+\ell^-$ through the decays $B \to K\ell^+\ell^-$ and $B \to K^*(892)\ell^+\ell^-$. Existing published upper limits come from CDF [4], and from earlier work by us [5]. Here we present improved upper limits.

The $B \to K^*\ell^+\ell^-$ decay rate peaks at low dilepton mass $m_{\ell\ell}$, due to the photon pole from $B \to K^*\gamma_{\text{virtual}}$, $\gamma_{\text{virtual}} \to \ell^+\ell^-$. [Throughout this Letter, the symbol K^* means $K^*(892)$.] Because the decay $B \to K^*\gamma$ is already well studied, and $|C_7|$ thus reasonably well known, we require $B \to K^*\ell^+\ell^-$ candidates to have dilepton mass above 0.5 GeV, to reduce the contribution from the virtual photon diagram and thus the dependence on $|C_7|$.

The data used in this analysis were taken with the CLEO detector [6] at the Cornell Electron Storage Ring (CESR), a symmetric e^+e^- collider operating in the $\Upsilon(4S)$ resonance region. The data sample consists of 9.2 fb^{-1} at the resonance, corresponding to 9.6×10^6 $B\bar{B}$ events, and 4.5 fb^{-1} at a center-of-mass energy 60 MeV below the resonance. The sample below the resonance provides information on the background from continuum processes $e^+e^- \to q\bar{q}$, $q = u, d, s, c$.

We search for $B \to K^{(*)}\ell^+\ell^-$ both in the $\mu^+\mu^-$ and e^+e^- modes, for $B \to K\ell^+\ell^-$ in both the $K^\pm$ and K^0 modes, and for $B \to K^*\ell^+\ell^-$ in the $K^{*0} \to K^+\pi^-$ and $K^0\pi^0$ modes and in the $K^{*\pm} \to K^\pm\pi^0$ and $K^0\pi^\pm$ modes, a total of 12 distinct final states. K^0 is detected via the $K^0 \to K_S^0 \to \pi^+\pi^-$ decay chain. We assume that the branching fractions for $B^+ \to K^+e^+e^-$, $B^+ \to K^+\mu^+\mu^-$, $B^0 \to K^0e^+e^-$, and $B^0 \to K^0\mu^+\mu^-$ all equal a common branching fraction $\mathcal{B}(B \to K\ell^+\ell^-)$ and that the branching fractions for $B^+ \to K^{*+}e^+e^-$, $B^+ \to K^{*+}\mu^+\mu^-$, $B^0 \to K^{*0}e^+e^-$, and $B^0 \to K^{*0}\mu^+\mu^-$ all equal a common branching fraction $\mathcal{B}(B \to K^*\ell^+\ell^-)$. We optimize our procedures to do the best job on $\mathcal{B}(B \to K\ell^+\ell^-)$ and $\mathcal{B}(B \to K^*\ell^+\ell^-)$, *not* on the individual modes and submodes.

There are three main sources of background: $B \to K^{(*)}\psi^{(\prime)}$, $\psi^{(\prime)} \to \ell^+\ell^-$, and other $B \to \psi^{(\prime)}X$ decays; continuum processes with two apparent leptons (either real leptons or hadrons misidentified as leptons); and $B\bar{B}$ decays other than $B \to \psi^{(\prime)}X$, with two apparent leptons. We suppress $B \to K^{(*)}\psi^{(\prime)}$ events with vetoes on the dilepton mass around ψ and ψ', in particular, $2.80 < m_{ee} < 3.23$ GeV, $2.90 < m_{\mu\mu} < 3.20$ GeV, $3.51 < m_{ee} < 3.77$ GeV, and $3.55 < m_{\mu\mu} < 3.74$ GeV. These very wide cuts are needed because of the low-side radiative tail from internal and external bremsstrahlung from $\psi^{(\prime)} \to e^+e^-$, and to a lesser extent the low-side radiative tail from internal bremsstrahlung from the $\mu^+\mu^-$ decay.

We suppress the background from $B\bar{B}$ semileptonic decays with a cut on the event missing energy, E_{miss}, since events with leptons from semileptonic B or D decay contain neutrinos. Distributions in E_{miss} for Monte Carlo samples of signal and background are shown in Fig. 1. We suppress continuum events with a cut on a Fisher discriminant, a linear combination of R_2 (the ratio of second and zeroth Fox-Wolfram moments [7] of the event), $\cos\theta_{tt}$ (θ_{tt} the angle between the thrust axis of the candidate B and the thrust axis of the rest of the event), S (the sphericity), and $\cos\theta_B$ (θ_B the production angle of the candidate B, relative to the beam direction). In particular, $\mathcal{F} = R_2 + 0.117|\cos\theta_{tt}| + 0.779(1 - S) + 0.104|\cos\theta_B|$. The coefficients of all terms but R_2 were determined by the standard Fisher discriminant procedure [8]. The relative weight
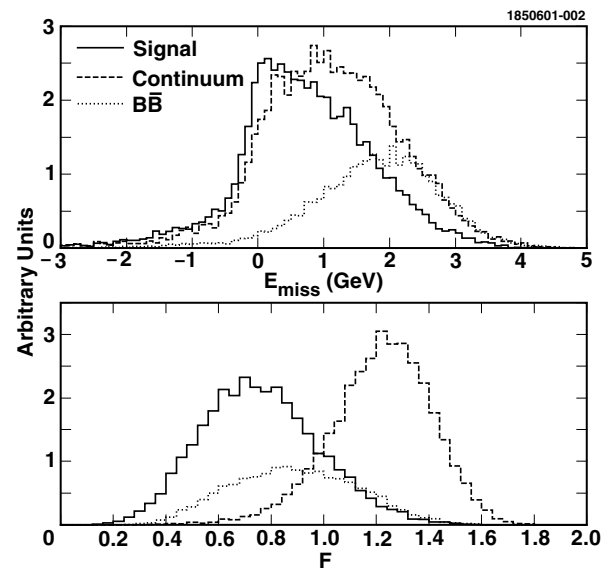

FIG. 1. Distributions in E_{miss} (upper panel) and $\mathcal{F}$ (lower panel) for Monte Carlo samples of signal events (solid line), $B\bar{B}$ background events (dotted line), and continuum background events (dashed line). The vertical scale is arbitrary.

given to R_2 was determined visually, from a scatter plot of R_2 vs the Fisher discriminant from the other three variables. Distributions in $\mathcal{F}$ for Monte Carlo samples of signal and background are shown in Fig. 1.

For those decay modes involving a charged kaon, we use specific ionization (dE/dX) and time-of-flight information to identify the kaon, cutting loosely (3 standard deviations) if those variables deviate from the mean for kaons in the direction away from the mean for pions, and harder (by a variable number, denoted kID^{cut}, of standard deviations) if they deviate on the side towards the pions.

All cuts have been determined from Monte Carlo samples: continuum events, $B\bar{B}$ events with no signal, and $B\bar{B}$ events with a $B \to K^{(*)}\ell^+\ell^-$ signal. We optimized cuts on $\mathcal{F}$, E_{miss}, and, where appropriate, kaon identification simultaneously. We found that the optimum curve in efficiency vs background space was traced out if we required that cuts on $\mathcal{F}$, E_{miss}, and kID were tightened or loosened together. In particular, we found that the optimum curve was well described by $E_{\mathrm{miss}}^{\mathrm{cut}} = 1.0 + 6.67 \times (\mathcal{F}^{\mathrm{cut}} - 0.8)$ GeV, $kID^{\mathrm{cut}} = 3.0 - 0.66 \times (3.0 - E_{\mathrm{miss}}^{\mathrm{cut}})$. With this formulation, we have a single cut variable, $\mathcal{F}^{\mathrm{cut}}$, to optimize.

We optimized the cuts to obtain either the best upper limit, assuming no signal, or to see the smallest possible signal. These two different optimization procedures led to similar cuts, and we took the average. In the optimization we allowed the value of $\mathcal{F}^{\mathrm{cut}}$ to vary from decay mode to mode, and optimize on $B \to K^{(*)}\ell^+\ell^-$, *not* on the individual modes. Thus, we have four (eight) $\mathcal{F}^{\mathrm{cut}}$'s to optimize jointly. We do this by stepping over a 4D (8D) grid in steps of 0.025. The final cuts on $\mathcal{F}$ are shown in Table I. The

corresponding cuts on E_{miss} and kID can be obtained from the expressions given above.

Our final discrimination between signal and background comes from the B reconstruction variables conventionally used for decays from the $\Upsilon(4S)$, beam-constrained mass $M_{\mathrm{cand}} \equiv \sqrt{E_{\mathrm{beam}}^2 - P_{\mathrm{cand}}^2}$ and $\Delta E \equiv E_{\mathrm{cand}} - E_{\mathrm{beam}}$. Our resolution in M_{cand} is 2.5 MeV, and in ΔE, 20 MeV. We define a signal box in $M_{\mathrm{cand}} - \Delta E$ space, ± 6.5 MeV around the B mass by ± 60 MeV ($\mu^+\mu^-$) or ± 70 MeV (e^+e^-) in ΔE. The signal box for e^+e^- events is shifted off zero by 5 MeV in ΔE, because radiation losses cause $B \to K^{(*)}e^+e^-$ signal events to peak at -5 MeV in ΔE rather than at zero.

The e^+e^- events suffer a degradation in resolution due to internal and external bremsstrahlung from the electrons. We partially recover that resolution by adding to each electron energy the energy of those photons found nearby in angle. This procedure improves the ψ veto, and resolution in E_{miss}, M_{cand}, and ΔE.

Background from $B \to \psi^{(\prime)}X$ is estimated from Monte Carlo simulation. Background from other B decay processes and from continuum processes is determined using a large sideband region in $M_{\mathrm{cand}} - \Delta E$ space: $5.20 < M_{\mathrm{cand}} < 5.29$ GeV, $|\Delta E| < 0.25$ GeV, but excluding the signal box. From Monte Carlo simulation, we found that the ratio of events in the signal region to events in the sideband region is 0.024 for $B\bar{B}$ background events other than $B \to \psi^{(\prime)}X$, and 0.027 for continuum background, in both cases smaller than the ratio of areas, 0.038, because backgrounds fall off as the candidate mass approaches the beam energy. Recognizing that this ratio must be larger for continuum background than for $B\bar{B}$ background because the

TABLE I. Value of $\mathcal{F}^{\mathrm{cut}}$, number of events observed in signal window, the expected background, efficiency (see text for definition), and upper limit on the branching fraction, for the 12 modes, and for $B \to K\ell^+\ell^-$, $B \to K^*\ell^+\ell^-$, and $0.65\mathcal{B}(B \to K\ell^+\ell^-) + 0.35\mathcal{B}(B \to K^*\ell^+\ell^-)$. Note the upper limits given in this table have been corrected for systematic error in background and efficiency.

Mode	$\mathcal{F}^{\mathrm{cut}}$	Observed events	Background	Efficiency	$\mathcal{B} \times 10^6$ upper lim.
$K^0 e^+ e^-$	0.938	1	0.10	0.053	8.45
$K^0 \mu^+ \mu^-$	0.925	0	0.21	0.041	6.64
$K^+ e^+ e^-$	0.925	1	0.95	0.165	2.40
$K^+ \mu^+ \mu^-$	0.850	1	0.74	0.111	3.68
$K\ell^+\ell^-$		3	1.99 ± 0.35	0.370	1.63
$K^0 \pi^+ e^+ e^-$	0.925	0	0.35	0.019	14.32
$K^0 \pi^+ \mu^+ \mu^-$	0.900	0	0.27	0.015	18.14
$K^+ \pi^0 e^+ e^-$	0.800	3	0.27	0.015	50.66
$K^+ \pi^0 \mu^+ \mu^-$	0.750	0	0.49	0.008	34.01
$K^+ \pi^- e^+ e^-$	0.925	1	0.97	0.071	5.58
$K^+ \pi^- \mu^+ \mu^-$	0.875	0	1.24	0.052	5.23
$K^0 \pi^0 e^+ e^-$	0.900	0	0.11	0.007	38.87
$K^0 \pi^0 \mu^+ \mu^-$	0.750	0	0.10	0.002	136.03
$K^*\ell^+\ell^-$		4	3.80 ± 0.57	0.189	3.26
Sum		7	5.79 ± 0.83	0.559	1.52

more jetlike continuum events will not fall off as rapidly as candidate mass approaches beam energy, and recognizing that using a lower background in an upper limit computation gives a more conservative answer, we take the continuum scaling factor to be equal to the $B\bar{B}$ scaling factor, rather than using 0.027.

The number of events that satisfy all cuts and land in the signal box is given, for each mode, in Table I, along with the background estimate. We find three $B \rightarrow K\ell^+\ell^-$ candidates, with an expected background of 2.0; we find four $B \rightarrow K^*\ell^+\ell^-$ candidates, with an expected background of 3.8. Thus there are a total of seven events with an expected background of 5.8. (The expected 5.8 background events are distributed 1.5 $B \rightarrow \psi'X$, 2.7 other B, 1.6 continuum.) The probability that a true mean of 5.8 will fluctuate up to seven or more events is 36%. Thus, there is no indication of signal. A scatter plot of M_{cand} vs ΔE for events passing all other cuts and landing in the signal or sideband region is shown in Fig. 2. Again, there is no indication of a signal. We obtain upper limits.

We calculate upper limits, at 90% confidence level, taking backgrounds into account. We use the pre–Feldman-Cousins formula [9]. To allow for the uncertainty in the background estimate, we use a value for the background which is reduced below our actual estimate. For $B \rightarrow K\ell^+\ell^-$ and $B \rightarrow K^*\ell^+\ell^-$ totals, we use the estimated background minus 1.28 standard deviations of its combined statistical and systematic error. (The factor 1.28 gives a 90% confidence level lower estimate of the background, assuming its uncertainty has a Gaussian distribution.) For individual modes, where backgrounds are

less precisely determined, we use half the estimated background. Results are given in Table I.

We gain experimental sensitivity to the underlying $b \rightarrow s\ell^+\ell^-$ interaction by calculating a weighted average over the two decay modes studied. To account for the difference in the experimental precision for each mode, we weight them by our relative efficiencies; that is, we compute an upper limit on the sum over all the individual submodes. This gives an upper limit on $0.65\mathcal{B}(B \rightarrow K\ell^+\ell^-) + 0.35\mathcal{B}(B \rightarrow K^*\ell^+\ell^-)$, where the coefficients 0.65 and 0.35 are the relative efficiencies we have for the two modes.

The efficiency for an individual submode, e.g., $B^+ \rightarrow K^{*+}\mu^+\mu^-$, $K^{*+} \rightarrow K^+\pi^0$, is defined as the number of detected events per $B^+ \rightarrow K^{*+}\mu^+\mu^-$ decay; i.e., the branching fraction for $K^{*+} \rightarrow K^+\pi^0$ is included in the efficiency, as are all K^* and K^0 decay branching fractions. The "efficiency" for $B \rightarrow K^{(*)}\ell^+\ell^-$ is the sum of the efficiency for the four (eight) contributing modes, and thus could, in principle, exceed 100%.

We use Monte Carlo simulation to determine the efficiency for detecting the signal modes. The decays $B \rightarrow K\ell^+\ell^-$ and $B \rightarrow K^*\ell^+\ell^-$ are generated using the model of Ali *et al.* [1]. The helicity of the K^* is taken into account. Final-state radiation is included, using the CERNLIB subroutine PHOTOS [10]. We have also generated decays with the two extreme variations that Ali *et al.* suggest for their model, and with several other models [1,11]. We find the model-to-model variation in efficiency to be small, with a relative rms variation of $\pm 3\%$.

To check our procedures, we have looked for the decays $B \rightarrow J/\psi K^{(*)}$ rather than vetoing them. We compare the branching fractions obtained with those from prior CLEO measurements. There is good agreement — differences are at or below the 1-standard-deviation level.

Systematic errors are of two varieties — those on the estimate of signal detection efficiencies and those on the estimate of backgrounds. The contributors to the former are lepton identification uncertainties (contributing $\pm 7\%$, relative, in the efficiency, for ee and $\mu\mu$ separately, $\pm 5\%$ for combined ee and $\mu\mu$), missing-energy-simulation uncertainties ($\pm 3.5\%$), and simulation uncertainties for M_{cand}, ΔE, dE/dX, time of flight, and $\mathcal{F}$ ($\pm 3.0\%$), giving a $\pm 7\%$ relative uncertainty in the overall efficiency. To this we add in quadrature $\pm 3\%$ for the model dependence of the efficiency, discussed earlier. The contributors to the background uncertainties are the modeling of $B \rightarrow \psi^{(l)}X$ ($\pm 10\%$) and uncertainties in the scale factors from sideband region to signal region in $M_{cand} - \Delta E$ space. We assign a systematic error to the $B\bar{B}$ background scale factor by determining it with different methods, obtaining 0.024 ± 0.004. Recognizing that the scale factor for continuum should be larger than that for $B\bar{B}$, we conservatively set it equal to the $B\bar{B}$ scale factor, with the same (correlated) systematic error. The errors shown on the backgrounds in Table I
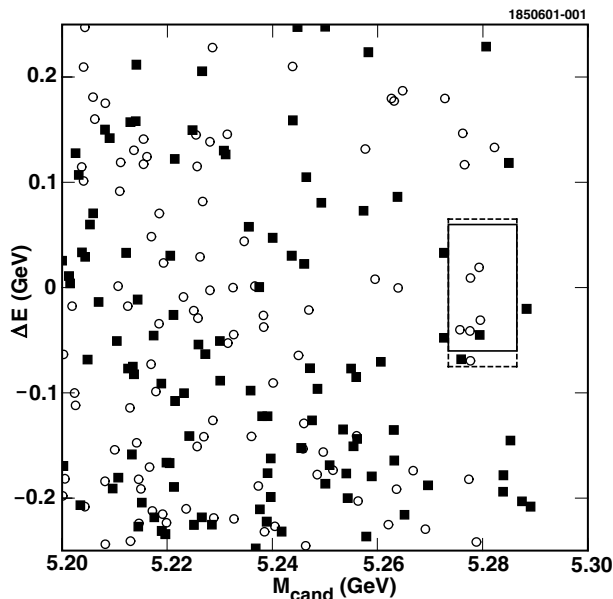

FIG. 2. Scatter plot of M_{cand} vs ΔE for ee events (open circles) and $\mu\mu$ events (solid squares) passing all other cuts, for data on the $\Upsilon(4S)$ resonance. The smaller box (solid squares) is the $\mu^+\mu^-$ signal box, while the larger box (dashed lines), shifted 5 MeV toward negative ΔE, is the e^+e^- signal box.

include statistical errors and the systematic errors just described.

There is no universally agreed-upon procedure for including systematic errors in upper-limit estimates. We conservatively reduce the background by 1.28 standard deviations and decrease the efficiency by 1.28 standard deviations. In this way we obtain our final results:

$$\mathcal{B}(B \to K\ell^+\ell^-) < 1.7 \times 10^{-6},$$

$$\mathcal{B}(B \to K^*(892)\ell^+\ell^-)_{m_{\ell\ell}>0.5 \text{ GeV}} < 3.3 \times 10^{-6}, \quad \text{and}$$

$$0.65\mathcal{B}(B \to K\ell^+\ell^-) +$$
$$0.35\mathcal{B}(B \to K^*(892)\ell^+\ell^-)_{m_{\ell\ell}>0.5 \text{ GeV}} < 1.5 \times 10^{-6},$$

all at 90% confidence level. These results are significant improvements over previously published limits [4,5].

The standard model values for these branching fractions, as given by Ali *et al.* [1], are 0.6×10^{-6} for $\mathcal{B}(B \to K\ell^+\ell^-)$ and 1.8×10^{-6} for $\mathcal{B}(B \to K^*\ell^+\ell^-)_{m_{\ell\ell}>0.5 \text{ GeV}}$, and thus 1.0×10^{-6} for the 0.65/0.35 weighted average. The limit on the branching fraction for $B \to K\ell^+\ell^-$ is therefore about 3 times its standard model prediction, the limit on the branching fraction for $B \to K^*\ell^+\ell^-$, subject to the requirement that $m_{\ell\ell} > 0.5$ GeV, is about twice its standard model prediction, and the 0.65/0.35 weighted average is only 50% larger than its standard model prediction.

In summary, we have searched for the decays $B \to K\ell^+\ell^-$ and $B \to K^*(892)\ell^+\ell^-$. We find no indication of a signal and obtain upper limits on the branching fractions. These limits are consistent with standard model predictions, but not far above them.

---

*Permanent address: Yonsei University, Seoul 120-749, Korea.
†Permanent address: University of Bergen, 5007 Bergen, Norway.

[1] A. Ali, P. Ball, L. T. Handoko, and G. Hiller, Phys. Rev. D **61**, 074024 (2000), and references therein; C. Greub, A. Ioannissian, and D. Wyler, Phys. Lett. B **346**, 149 (1995).

[2] CLEO Collaboration, R. Ammar *et al.,* Phys. Rev. Lett. **71**, 674 (1993).

[3] CLEO Collaboration, M. S. Alam *et al.,* Phys. Rev. Lett. **74**, 2885 (1995).

[4] CDF Collaboration, T. Affolder *et al.,* Phys. Rev. Lett. **83**, 3378 (1999).

[5] T. Skwarnicki, in *Proceedings of the XXIXth International Conference on High Energy Physics, Vancouver, Canada, 1998,* edited by A. Astbury, D. Axen, and J. Robinson (World Scientific, Singapore, 1999), p. 1057; CLEO Collaboration, S. Glenn *et al.,* Phys. Rev. Lett. **80**, 2289 (1998).

[6] CLEO Collaboration, Y. Kubota *et al.,* Nucl. Instrum. Methods Phys. Res., Sect. A **320**, 66 (1992); T. Hill, Nucl. Instrum. Methods Phys. Res., Sect. A **418**, 32 (1998).

[7] G. Fox and S. Wolfram, Phys. Rev. Lett. **41**, 1581 (1978).

[8] R. A. Fisher, Ann. Eugen. **7**, 179 (1936); M. C. Kendall and A. Stuart, *The Advanced Theory of Statistics* (Hafner, New York, 1968), 2nd ed., Vol. III.

[9] Particle Data Group, R. M. Barnett *et al.,* Phys. Rev. D **54**, Part I, 1 (1996).

[10] E. Barberio and Z. Was, Comput. Phys. Commun. **79**, 291 (1994).

[11] P. Ball and V. M. Braun, Phys. Rev. D **58**, 094016 (1998); Patricia Ball, J. High Energy Phys. **9809**, 005 (1998); D. Melikhov and N. Nikitin, hep-ph/9609503; P. Colangelo *et al.,* Phys. Rev. D **53**, 3672 (1996); Phys. Rev. D **57**, 3186(E) (1998).